

SALT : Subspace Alignment as an Auxiliary Learning Task for Domain Adaptation

Kowshik Thopalli[†], Jayaraman J. Thiagarajan[‡], Rushil Anirudh[‡], Pavan Turaga[†]

[†]Arizona State University, [‡]Lawrence Livermore National Labs

Abstract

Unsupervised domain adaptation aims to transfer and adapt knowledge learned from a labeled source domain to an unlabeled target domain. Key components of unsupervised domain adaptation include: (a) maximizing performance on the target, and (b) aligning the source and target domains. Traditionally, these tasks have either been considered as separate, or assumed to be implicitly addressed together with high-capacity feature extractors. When considered separately, alignment is usually viewed as a problem of aligning data distributions, either through geometric approaches such as subspace alignment or through distributional alignment such as optimal transport. This paper represents a hybrid approach, where we assume simplified data geometry in the form of subspaces, and consider alignment as an auxiliary task to the primary task of maximizing performance on the source. The alignment is made rather simple by leveraging tractable data geometry in the form of subspaces. We synergistically allow certain parameters derived from the closed-form auxiliary solution, to be affected by gradients from the primary task. The proposed approach represents a unique fusion of geometric and model-based alignment with gradients from a data-driven primary task. Our approach termed SALT, is a simple framework that achieves comparable or sometimes outperforms state-of-the-art on multiple standard benchmarks.

the covariate shift is available. The covariate shift commonly considered in unsupervised domain adaptation formulations assume that the distributions on source and target domains differ only in their marginal feature distributions $P(X)$ while having an identical conditional distribution $P(y|X)$, where X and y are correspond to features and labels from either the source (X_s, y_s) or target (X_t, y_t) domains.

More successful solutions for domain adaptation attempt to infer domain-invariant data representations by directly minimizing the discrepancy between the marginal feature distributions from the two domains. For example, domain adversarial learning, which seeks to find a common representation where the two domains are indistinguishable, is at the core of several state-of-the-art methods [49, 16, 29, 9, 10]. However, it has recently been shown that domain adversarial training can be ineffective when working with a high-capacity feature extractor [43]. High-capacity networks allow for learning arbitrary transformations that can reduce domain mismatch in terms of marginal feature distributions, yet might have no bearing on the final classifier performance [43]. This has motivated the inclusion of a variety of consistency-enforcing losses into the domain adversarial learning formulation to regularize the learning process. For example, both feature and semantic losses for feature-level adaptation may be employed [10, 49], while pixel-level adaptation via pixel and semantic consistency losses may also be employed [25, 3]. More recently, Hoffman *et. al.* [16] proposed to enforce cyclical consistency based on all the aforementioned losses, while Shu *et. al.* [43] introduced a virtual adversarial loss to better regularize domain adversarial learning.

1. Introduction

Despite significant advances in neural network architectures and optimization strategies for supervised learning, one of the long-standing challenges has been to effectively generalize classifier models to novel testing scenarios, typically characterized by unknown covariate shifts [15] or changes in label distributions. In this paper, we consider the problem of *unsupervised domain adaptation*, wherein the goal is to utilize labeled data from a *source* domain to design a classifier that can generalize to an unlabeled *target* domain. We are especially interested in the case when no knowledge about

Key insights: The above discussion leads us to our core idea that the process of minimizing domain discrepancies, while also learning a highly generalizable classifier, could be potentially regularized by adopting alignment methods with simplified data geometries. A natural candidate is subspace alignment [5, 11, 42, 47], which utilizes simplified data representations, i.e., low-dimensional linear subspaces, and poses the problem of achieving domain invariance as learning a mapping between those representations. Despite

their mathematical tractability, these methods are typically agnostic to the end-task and rely on modeling assumptions that are insufficient to describe complex datasets. Thus, they perform poorly in comparison to more recent approaches in domain adaptation. Consequently, one must attempt to blend the representational convenience of simplified data geometries, while not being constrained by the limited capabilities of these methods.

To this end, we develop SALT, an unsupervised domain adaptation algorithm based on simple subspace-based alignment, which is capable of producing highly effective classifiers through synergistic optimization between improving classifier performance and minimizing domain mismatch. Intuitively, by handling the interactions between domain alignment and end-task objectives, we simultaneously regularize the domain adaptation process and eliminate the commonly observed performance limitations of subspace-based methods.

Contributions and findings: In this paper, we cast explicit domain alignment as an *auxiliary* task, whose fidelity can be carefully adjusted to maximize the quality of the primary task, i.e., performance of the classifier on both source and target domains. More specifically, we define *adaptable subspace alignment* as the auxiliary task, which uses gradients from the primary task, to adjust the domain alignment. We show that even with a simplified global subspace alignment model, SALT yields a comparable or sometimes higher adaptation performance than even state-of-the-art methods with sophisticated adaptation strategies. Our major findings are:

- With a disjoint primary-auxiliary formulation, we find that even a naïve global subspace based alignment [5] with a *fixed* feature extractor, achieves higher or similar performance compared to state-of-the-art approaches on several benchmarks.
- By viewing domain alignment as an auxiliary task, we are able to entirely dispense the need for adversarial learning, consistency-enforcing regularizers, and other extensive hyper-parameter choices.
- We find SALT to be robust to varying data availability in the target domain, which can be attributed to the simplified data representations used for alignment.
- Though SALT uses only linear subspaces for alignment, we are able to increase its complexity through the use of an ensemble of subspace models and achieve improved performance.

2. Related work

Unsupervised domain adaptation: Unsupervised domain adaptation has been an important problem of research in multiple application areas and a wide variety of solutions have been developed. Earlier works focused on adapting

the features of source and target domains by minimizing statistical divergence between them [38, 11, 34, 44, 6, 45]. These works can be analyzed through the foundational work of Ben David *et. al.* [1], which provides an upper bound on target error, $\epsilon(\mathcal{D}_T; h)$ on target data \mathcal{D}_T , that can be achieved using a hypothesis h as the sum of three terms:

$$\epsilon(\mathcal{D}_T; h) \leq \mathcal{L}(\mathcal{D}_S; h) + \mathcal{L}_{\mathcal{H}}(\mathcal{D}_S, \mathcal{D}_T) + \mathcal{L}_{\delta}(h), \quad (1)$$

where, the first term denotes the error in the source domain \mathcal{S} , the second term is the discrepancy between the source-target pair (\mathcal{H} -divergence), and the third term measures the optimal error achievable in both the domains (often assumed to be negligible). Under this context, there are two broad categories of methods – ones that assume there exists a single hypothesis h that can perform well in both domains (*conservative*), and those that do not make that assumption (*non-conservative*) [43]. Successful state-of-the-art methods use powerful feature extractors such as convolutional neural networks (CNNs), and aim to jointly minimize source error along with domain divergence error. Adversarial learning [12] has been the workhorse of these solutions, implemented with different additional regularizers [10, 29, 16, 24, 18].

Subspace-based alignment: The key idea behind this class of methods is to represent source and target data distributions on lower-dimensional subspaces, align the subspaces, and subsequently project the target data onto the aligned subspace. A classifier is finally trained on the newly computed lower dimensional source data and evaluated on target data. Popular approaches include [11, 13, 5, 45]. Geodesic-based methods [13, 11] compute a path along the manifold of subspaces (Grassmannian), and either project the source and target onto points along that path [13] or compute a linear map that projects source samples directly onto the target subspace [11]. Furthermore, works such as [5, 45] align the source and target subspaces using Procrustes methods [5], or by considering distributional statistics along with subspace basis [45].

Meta auxiliary learning: Meta-learning has been a recently successful approach in generalizing knowledge across related tasks [7]. Broadly, meta-learning techniques can be grouped into three categories [7] – metric-based [21, 51], model-based [41, 32] and optimization-based [7, 36]. Auxiliary learning on the other hand essentially focuses on increasing the performance of a primary task through the help of another related auxiliary task(s). This methodology has been applied to areas such as speech recognition [48], depth estimation, semantic segmentation [23], and reinforcement learning [19]. The work closely related to ours is *meta-auxiliary learning* [26], which aims to improve m -class image classification performance (primary task) by solving a k -class classification problem (auxiliary task). This is done by establishing a functional relationship between the classes.

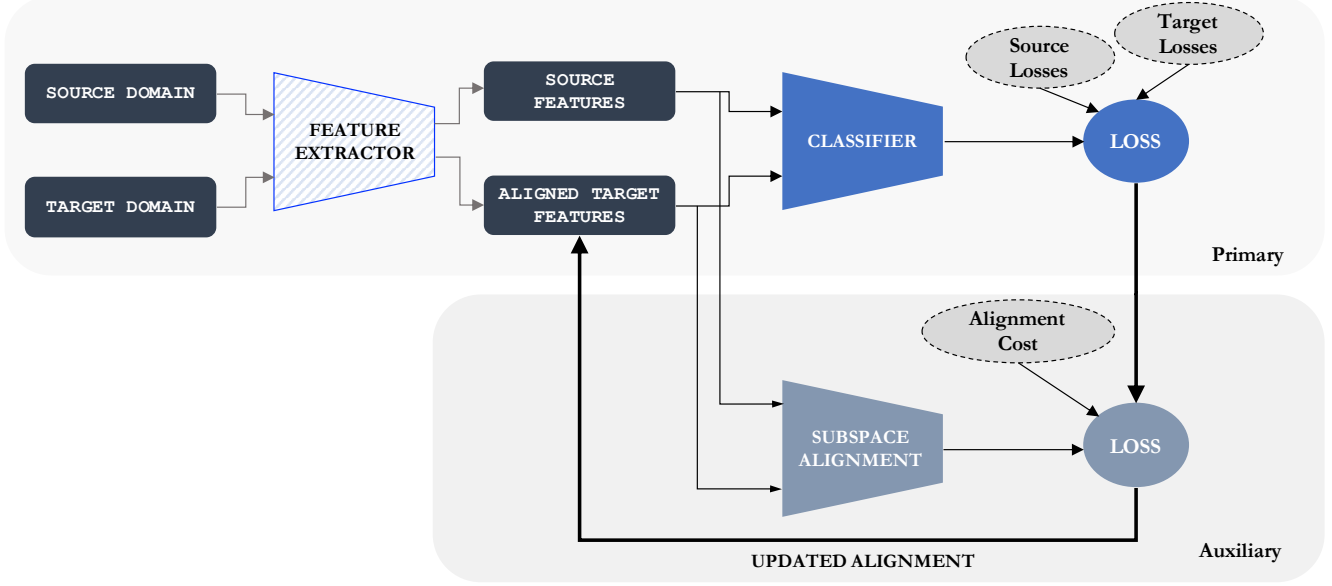


Figure 1: An overview of the proposed approach for unsupervised domain adaptation. We leverage gradients from the *primary task* of designing a generalizable classifier to guide the domain alignment, which is posed as an *auxiliary task*. While the primary task utilizes deep neural networks, the auxiliary task is carried out using a simplified data geometry – subspaces – in lieu of adversarial training or sophisticated distribution matching. Note, even the *feature extractor* is frozen after an initial training phase.

In contrast, we formulate subspace-based domain alignment as the auxiliary to the primary task of building a classifier that works well in both source and target domains.

3. Proposed Approach

In this section, we describe the proposed method for unsupervised domain adaptation. An overview of the approach can be found in Figure 1. We assume access to data from the labeled source and unlabeled target domains, \mathcal{D}_S and \mathcal{D}_T denoted as $\{X_s, y_s\}$ and $\{X_t\}$ respectively. In the rest of this paper, we use X_s, X_t to indicate the latent features for source and target domains from a pre-trained feature extractor, \mathcal{F} , such as ResNet50 [14]. The primary network updates the classifier given the source and current best estimate of source-aligned target features, such that the inferred model is effective for both source and target domains. The auxiliary network solves for subspace-based domain alignment, while minimizing both the alignment cost, and the loss from the primary network. Though the resulting alignment is sub-optimal in terms of the pure alignment cost, it is optimal when conditioned on the primary classification task.

3.1. Primary Task: Classifier design

We construct the primary task with the goal of achieving effective class discrimination in both source and target domains. With inputs as source/target images directly, or latent features extracted from a pre-trained feature extractor \mathcal{F} , we learn the parameters for a classifier network \mathcal{P}_Θ parameterized by Θ . The losses used for

the optimization include: (i) standard categorical cross-entropy loss $\mathcal{L}_y(\Theta; \mathcal{D}_S) = \mathbb{E}_{x, y \sim \mathcal{D}_S} [y^\top \ln \mathcal{P}_\Theta(x)]$ for the labeled source data, (ii) conditional entropy [43] loss on the softmax predictions for target data $\mathcal{L}_c(\Theta; \mathcal{D}_T) = -\mathbb{E}_{x \sim \mathcal{D}_T} [\mathcal{P}_\Theta(\mathcal{A}_\Phi(x))^\top \ln \mathcal{P}_\Theta(\mathcal{A}_\Phi(x))]$, and (iii) class-balance loss [8] for the unlabeled target domain \mathcal{L}_{cb} , which is implemented as binary cross-entropy loss between the mean prediction from the network over a mini-batch to that of a uniform probability vector – this loss regularizes network behavior when the data exhibits large class imbalance. Note that, in the definition of \mathcal{L}_c , the target domain features are first transformed using the auxiliary network \mathcal{A}_Φ (defined in Section 3.2) prior to applying the classifier. The overall loss function is thus defined as

$$\mathcal{L}_P = \mathcal{L}_y + \lambda_c \mathcal{L}_c + \lambda_{cb} \mathcal{L}_{cb}. \quad (2)$$

Here, the second and third terms are used as regularizers to counter the assumption that a single hypothesis h might not be effective for both domains, *i.e.* non-conservative.

3.2. Auxiliary Task: Domain alignment

We posit that an alternating optimization between a generalizable classification task, and an auxiliary domain alignment task, relaxes the requirements of the alignment step such that even simple alignment strategies can provide sufficient information to improve the classifier. In order to test this idea, we assume a simplified data geometry, in the form of low-dimensional linear subspaces [5]. Note that, as a generative model for a dataset, a single linear subspace or

even a union of linear subspaces is a poor choice on its own. However, when coupled with an appropriate primary task using a sufficiently high capacity classifier, we will show it can be highly effective in domain adaptation. Though we report results only with subspace-based domain alignment, without loss of generality, the same algorithm can be extended to other domain alignment approaches including domain adversarial training [27], optimal transport [4] etc.

Closed-form subspace alignment: Let us denote the basis vectors for the d -dimensional subspaces inferred from source and target domains as $\{Z_s\}$ and $\{Z_t\}$ respectively and they satisfy $Z_s^T Z_s = \mathbb{I}$, $Z_t^T Z_t = \mathbb{I}$, where \mathbb{I} denotes the identity matrix. The subspaces are inferred using singular value decomposition of source/target domain latent features $\{X_s, X_t\}$. The alignment between two subspaces can be parameterized as an affine transformation Φ , *i.e.*

$$\Phi^* = \arg \min_{\Phi} \|Z_t \Phi - Z_s\|_F^2, \quad (3)$$

where, $\|\cdot\|_F$ denotes the Frobenius norm. The solution to this alignment cost (3) can be obtained in closed-form [5] as

$$\Phi^* = (Z_t)^T Z_s. \quad (4)$$

This implies that the adjusted coordinate system, also referred as the *source-aligned target subspace* can be constructed as

$$Z_t^a = Z_t (Z_t)^T Z_s. \quad (5)$$

Though we develop our formulation by aligning the target subspace onto the source, without loss of generality, one can equivalently project the source subspace onto the target. Since the primary task invokes the classifier optimization using features in the ambient space, we need to re-project the target features using Z_t^a , *i.e.*

$$\begin{aligned} \hat{X}_t^* &= \arg \min_{\hat{X}_t} \left\| \hat{X}_t Z_s - \hat{X}_t Z_t^a \right\|_F^2 \\ &= \arg \min_{\hat{X}_t} \left\| \hat{X}_t Z_s - \hat{X}_t Z_t (Z_t)^T Z_s \right\|_F^2, \end{aligned} \quad (6)$$

where \hat{X}_t^* denotes the modified target features. The solution to this optimization can be obtained in closed-form as

$$\mathcal{A}_{\Phi}(X_t) = \hat{X}_t^* = X_t Z_t \Phi^* Z_s^T, \quad (7)$$

where Φ^* is computed using (4).

Task-dependent tuning of subspace alignment: Since the overall objective is to refine the auxiliary network parameters to maximally support the primary task, we propose to include the terms \mathcal{L}_c and \mathcal{L}_{cb} from (2) to the alignment objective in (3),

$$\mathcal{L}_{\mathcal{A}} = \|Z_t \Phi - Z_s\|_F^2 + \gamma_c \mathcal{L}_c + \gamma_{cb} \mathcal{L}_{cb}. \quad (8)$$

Note that, when we make this modification, there no longer exists a closed-form solution. Hence, we adopt an approach

Algorithm 1: SALT for unsupervised domain adaptation.

Input: Labeled source features $\{X_s, y_s\}$ and unlabeled target features $\{X_t\}$ from \mathcal{F} . Source and target subspaces $Z_s; Z_t$

Initialize: Random state for Θ , Alignment Φ using (4).

Hyper-parameters $\lambda_c, \lambda_{cb}, \gamma_c, \gamma_{cb}, n_{iter}, T_1, T_2$.

Training Phase:

Split: $X_s^{\dagger}, X_s^{\ddagger} \leftarrow X_s$ and $X_t^{\dagger}, X_t^{\ddagger} \leftarrow X_t$

for $iter$ **in** n_{iter} **do**

 // update \mathcal{P}_{Θ}

for t_1 **in** T_1 **do**

 Compute $\hat{X}_t^{\dagger} = X_t^{\dagger} Z_t \Phi^* Z_s^T$ following (7);

$\hat{y}_s^{\dagger} = \mathcal{P}_{\Theta}(\hat{X}_s^{\dagger})$;

$\hat{y}_t^{\dagger} = \mathcal{P}_{\Theta}(\hat{X}_t^{\dagger})$;

 Compute $\mathcal{L}_{\mathcal{P}}$ using (2);

 Update $\Theta^* = \arg \min_{\Theta} \mathcal{L}_{\mathcal{P}}$;

end

 // update \mathcal{A}_{Φ}

for t_2 **in** T_2 **do**

 Compute \hat{X}_t^{\ddagger} using (7);

 Compute $\hat{y}_t^{\ddagger} = \mathcal{P}_{\Theta^*}(\hat{X}_t^{\ddagger})$;

 Compute $\mathcal{L}_{\mathcal{A}}$ using (8);

 Update $\Phi^* = \arg \min_{\Phi} \mathcal{L}_{\mathcal{A}_{\Phi}}$;

end

end

that takes in gradients from the primary task to adjust Φ . To enable this end-to-end training of both the primary and auxiliary tasks, we implement *subspace alignment* as a network \mathcal{A} that parameterizes Φ as a fully connected layer of d neurons without any non-linear activation function or bias.

Objective: The overall objective of this primary-auxiliary network learning can be formally written as the following bi-level optimization problem:

$$\min_{\Theta} \mathcal{L}_{\mathcal{P}}(\Theta; X_s, y_s, \mathcal{A}_{\Phi^*}(X_t)), \quad (9)$$

$$\text{where, } \Phi^* = \arg \min_{\Phi} \mathcal{L}_{\mathcal{A}}\left(\Phi; Z_s, Z_t, \mathcal{P}_{\Theta}(\mathcal{A}_{\Phi}(X_t))\right).$$

We now describe the algorithm for solving this objective.

3.3. Algorithm

Given the primary and auxiliary task formulations, one can adopt different training strategies to combine their estimates: (i) *Independent*: This is the classical approach, where the alignment obtained by solving (3) is used to infer the classifier parameters, (ii) *Joint*: This jointly optimizes for both networks together, similar to existing domain adaptation methods, (iii) *Alternating*: This alternating style of optimization solves for the primary task with the current

Method	I \rightarrow P	P \rightarrow I	I \rightarrow C	C \rightarrow I	C \rightarrow P	P \rightarrow C	Average
No Adaptation	76.5	88.2	93	84.3	69.1	91.2	83.7
DAN [27]	74.5	82.2	92.8	86.3	69.2	89.8	82.5
DANN [10]	75.0	86.0	96.2	87.0	74.3	91.5	85.0
JAN [30]	76.8	88.0	94.7	89.5	74.2	91.7	85.8
CDAN+E [29]	78	90.9	98.1	91.6	74.4	94.6	87.9
SALT	80.16	95.5	97.3	90.9	79.3	97	90.02

Table 1: Classification accuracy on the ImageCLEF dataset. Best performance is shown in **bold**, and the second best in **bold italic**.

estimate of the alignment, and subsequently updates the auxiliary network with both primary and auxiliary losses. As we will show later, that this alternating optimization strategy works the best in comparison to the other two. We now describe the alternating optimization strategy.

Initialization phase: The choice of initial states for the parameters of both the primary and auxiliary networks is crucial to the performance of our algorithm. First, we pre-train the feature extractor \mathcal{F} and the classifier \mathcal{P}_Θ using the loss function (2) without any explicit domain alignment. We then fit d -dimensional subspaces, Z_s and Z_t , to the features obtained using \mathcal{F} for both the source and target domains. Note that the feature extractor is not updated for the rest of the training process, and hence the subspace estimates are fixed. The initial state of Φ , *i.e.* alignment matrix between the two subspaces, is obtained using (4).

Training phase: In order to enable information flow between the two tasks, we propose to allow the auxiliary task to utilize gradients from the primary task. Similarly, the estimated alignment is applied to the target data while updating the classifier parameters in the primary task. The auxiliary loss construction described in Section 3.2 provides a link between the primary and auxiliary tasks.

The primary and auxiliary tasks are solved alternatively until convergence – during the auxiliary task optimization, we freeze the classifier parameters and update \mathcal{A}_Φ using equation (8). Since the feature extractor \mathcal{F} is fixed, there is no need to recompute the subspaces. In our implementation we find that optimizing the auxiliary task using a held-out validation set, distinct from that used for the primary task, leads to significant performance improvements. Given the estimate for Φ , we freeze the auxiliary network \mathcal{A}_Φ and update the classifier network using source features and source-aligned target features to minimize the primary loss in (2). Upon convergence (typically within 5 – 10 iterations on all datasets considered), optimal values for both Φ and \mathcal{P}_Θ are returned. A detailed listing of this process is provided in algorithm 1.

Using an ensemble of subspaces: The fidelity of the auxiliary task relies directly on the quality of the subspace ap-

proximation. For complex datasets, a single low-dimensional subspace is often a poor approximation. Hence, we propose to allow the complexity of the auxiliary model to be adjusted through the use of multiple target subspaces. To this end, we obtain independent bootstraps of the target data and fit a single low-dimensional subspace of dimension d to each of them. While solving for the auxiliary task, we compute individual alignment matrices to the source with respect to the same classifier \mathcal{P}_Θ . During the update of the classifier \mathcal{P}_Θ , we pose this as a multi-task learning problem, wherein a single classifier is used with different source-aligned targets. This is valid since all (bootstrapped) subspaces are in the same ambient feature space. During test time, we treat the predictions obtained using features from different alignment matrices as an ensemble and perform majority voting for making the final prediction.

4. Experiments

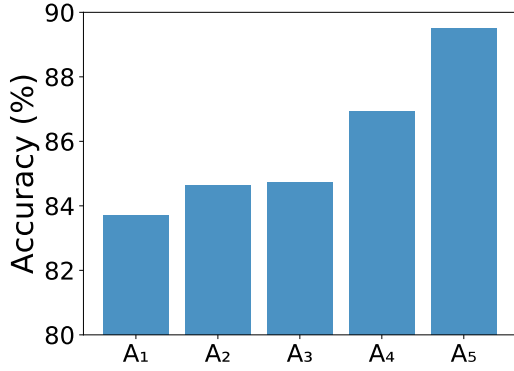
We evaluated the proposed method on four widely used visual domain adaptation tasks – digits, ImageCLEF, VisDA-2017 challenge, and Office-Home datasets, and present comparisons to several state-of-the-art domain adaptation techniques. Across all the experiments, an 80-20 random split of source and target training data was performed to update the primary and auxiliary tasks. All experiments were run using the PyTorch framework [35] with a Nvidia-TitanX GPU.

4.1. ImageCLEF-DA

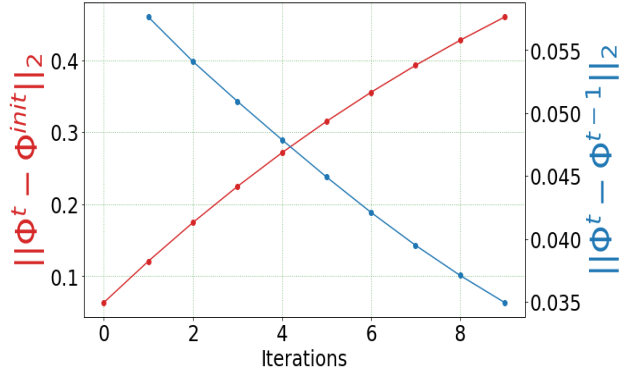
Dataset: ImageCLEF¹ is organized by selecting common categories of images shared by three public image datasets (domains): *ImageNet ILSVRC 2012* (**I**), *Caltech-256* (**C**), and *Pascal VOC 2012* (**P**). There are 12 categories, with 50 images each, resulting in a total of 600 images in each domain. We conduct 6 experiments by permuting the 3 domains : **I** \rightarrow **P**, **P** \rightarrow **I**, **I** \rightarrow **C**, **C** \rightarrow **I**, **C** \rightarrow **P**, **P** \rightarrow **C**.

Model: Our feature extractor is based on the pre-trained ResNet-50 architecture [14, 37]. This model is then fine-tuned w.r.t loss computed from (2), with $\Phi = \mathbb{I}$, where \mathbb{I}

¹<http://imageclef.org/2014/adaptation>



(a) Ablation study



(b) Dynamics of Φ across iterations

Figure 2: (a) Ablating different components in the proposed method against adaptation performance on the ImageCLEF dataset. See text in Section 4.1 for notation. (b) Changes in Φ from Φ^{init} (4) across iterations are represented by the red Curve while the blue curve denotes successive differences in Φ

is identity, and λ_c and λ_{cb} set at 0.1. We then use SALT on the latent features from the penultimate layer of the fine-tuned ResNet. Source and target subspaces of dimension 800 are constructed from these 2048-dimensional features using SVD. The classifier network is chosen to be the last fully connected layer, subsequently refined using the SGD optimizer with the learning rate $1e-4$ and momentum 0.9. The subspace alignment network is trained with a learning rate of $1e-3$ using the Adam optimizer [20]. The proposed approach is compared against a number of baseline methods including [29, 27, 10, 30] and the results are reported in Table 1. The results clearly show that even a naïve global alignment strategy improves performance by nearly 3 percentage points over sophisticated adversarial learning methods, with SALT’s alternating optimization strategy.

Ablation Study: In order to understand the impact of the different components, we perform an ablation study on this dataset. We describe each setting in this experiment next:

- A₁ No Adaptation:** A baseline method where we use the classifier trained on the source directly on the target features without any adaptation.
- A₂ Primary Only:** We leave out the auxiliary task, but include all the losses used in the primary task described in equation (2), with $\mathcal{A}_\Phi = \mathbb{I}$.
- A₃ Independent:** Here, we use the closed form solution in subspace alignment from equation (5), and then solve for the primary task in (2) independently.
- A₄ Joint Optimization:** We employ a joint optimization strategy, wherein we jointly update the alignment Φ , and the classifier together.
- A₅ Alternating Optimization:** This is our proposed strategy that updates Φ and the classifier in an alternating fashion.

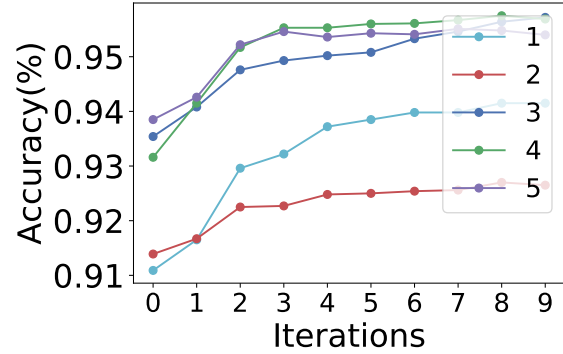


Figure 3: *SVHN* → *MNIST* DA task - Effect of using an ensemble of target subspaces on the performance of SALT.

The results from the study are illustrated in Figure 2(a). A key observation is that, since the alignment strategy is weak, when done independently it does not lead to any performance gains. However, the proposed optimization provides significant improvement over even a joint optimization strategy.

Convergence of Φ : Through Figure 2(b) we report the training behavior of the alignment matrix Φ returned by the auxiliary network \mathcal{A}_Φ . While the red curve in Figure 2(b) indicates the change in Φ across iterations indexed by t w.r.t the closed form solution Φ^{init} obtained in (4), the blue curve represents the successive difference in Φ across iterations. As expected, the estimate for Φ changes non-trivially from Φ^{init} , eventually converging to a solution that leads to maximal classification performance. Note, in all our experiments, we find that the Φ returned by the auxiliary network is always a well-conditioned, full rank matrix.

Method	MNIST→ USPS	USPS→ MNIST	SVHN→ MNIST
No Adaptation	94.8	49	60.7
DeepCoRAL [46]	89.3	91.5	59.6
MMD [28]	88.5	73.5	64.8
DANN [10]	95.7	90.0	70.8
ADDA [49]	92.4	93.8	76.0
DeepJdot [2]	95.6	96.0	96.7
CyCADA [16]	95.6	96.5	90.9
UNIT [24]	95.9	93.5	90.5
GenToAdapt [40]	95.3	90.8	92.4
SALT	96.2	97.4	95.6

(a) Digits datasets

Method	Average Accuracy
No Adaptation	54.2
JAN [30]	61.6
CDAN [29]	70.2
SALT	76.3

(b) VISDA-2017

Table 2: Performance of the proposed method on Digits and VISDA datasets. We highlight the best performing technique in **bold**, and the second best in **bold italic**.

4.2. Digits classification

Datasets: We consider three data sources for the digits classification task: USPS [17], MNIST [22], and the Street View House Numbers (SVHN) [33] datasets. Each of these datasets have 10 categories (digits from 0-9). We perform the following three experiments in this task. a) MNIST → USPS, b) USPS → MNIST, and c) SVHN → MNIST and report the accuracies on the standard target test sets.

Model: The model used for all the 3 tasks is based on the architecture from [2], which is comprised of six 3×3 convolutional layers containing $\{32, 32, 64, 64, 128, 128\}$ filters with ReLU activations and two fully-connected layers of 128 and 10 (number of classes) hidden units. The Adam optimizer ($lr = 2e^{-4}$) was used to update the model using a mini-batch size of 512 for the two domains. We compare our results with a number of state-of-the-art domain adaptation methods and the results are shown in Table 2. SALT achieves the highest accuracy averaged across all three digits datasets, beating state-of-the-art in two out of three cases, and second highest marginally below DeepJDOT [2], in the case of SVHN → MNIST.

With one of the tasks in this dataset, we also study the effect of using multiple subspaces on the classification per-

formance. As discussed earlier, allowing multiple target subspaces increases the complexity of the auxiliary task. As showed in Figure 3, with the SVHN → MNIST DA task, using 3 or more subspaces leads to significant performance gains. However, we found that increasing it further did not lead to additional improvements.

4.3. VisDA-2017

Dataset: VisDA-2017 is a difficult simulation-to-realworld dataset with two highly distinct domains: *Synthetic*, renderings of 3D models from different angles and with different lightning conditions; *Real* which are natural images. This dataset contains over 280K images across 12 classes.

Model: Given the dataset complexity, we choose the pre-trained ResNet-152 [14] as our feature extractor and as in previous case, we fine tune it to obtain the 2048-dimensional features and the subspace dimension is 800. The classifier and subspace alignment networks are trained with the same hyper-parameters as in Section 4.1. From Table 2b, it can be seen that our model comprehensively outperforms the results reported so far in the literature, by six percentage points.

4.4. Office-Home

Datasets: This challenging dataset [50] contains 15,500 images in 65 classes from office and home settings, forming 4 extremely dissimilar domains: Artistic images (**Ar**), Clip Art (**Cl**), Product images (**Pr**), and Real-World images (**Rw**).

Model: Similar to Section 4.1, we fine tune a pre-trained ResNet-50 and obtain the 2048-dimensional features, and build subspaces of 800 dimensions. The classifier and auxiliary networks are trained with the same hyper-parameters as earlier. Comparisons to the state-of-the-art methods can be found in Table 3. We observe that while SALT consistently outperforms baseline methods including the recent DeepJdot [2], with comparable performance to the highest reported – CDAN [29] in terms of the average accuracy across all pairs of DA tasks (see Supplementary for detailed results).

Method	Average Accuracy
No Adaptation	59.7
DeepJdot [2]	50.6
DAN [27]	56.3
DANN [10]	57.6
JAN [30]	58.3
CDAN [29]	65.8
SALT	65.1

Table 3: Classification accuracy on Office-Home dataset. Best performance is shown in **bold**, and the second best in **bold italic**.

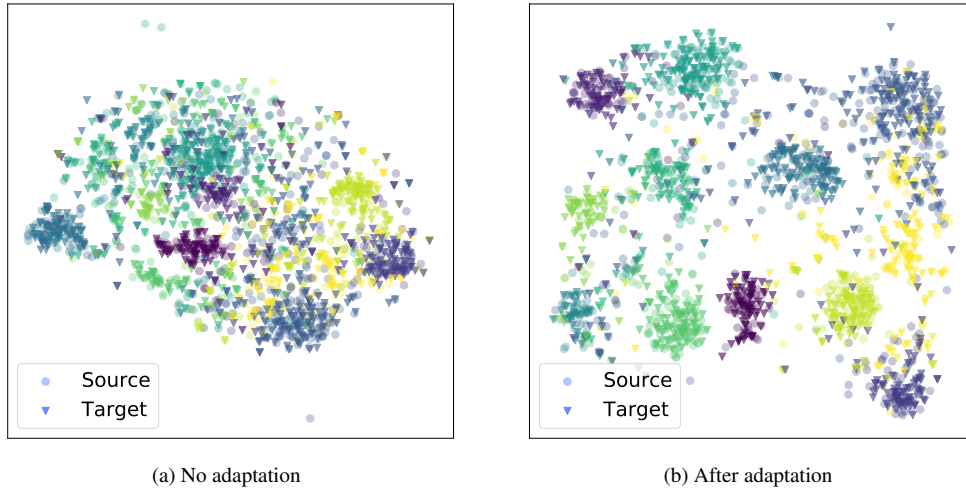


Figure 4: *VisDA-2017* - Visualizing the adaptation across source and target domains using t-SNE [31]. We observe improved alignment between the class boundaries of the source and target domains.

4.5. SALT relaxes data requirements

Owing to its design simplicity, we surmise that SALT admits improved data efficiency. To test this hypothesis, we evaluate SALT under the scenario where the amount of unlabeled target data is limited. While we perform SALT with varying target data sizes, we report accuracies on the full target test set. In particular, we consider the problem of adapting USPS \rightarrow MNIST and the results from 3 random trials are shown in Figure 5. It can be seen that even with 30% lesser training data in the target domain, SALT still outperforms state-of-the-art baselines that have access to the entire data. Further, the drop in performance even when operating at only 50% of data is very low ($\approx 2\%$ points), thus evidencing that a simpler alignment strategy can reduce the data requirements while not compromising the performance.

5. Conclusions

In this work, we present a principled and effective approach to tackle the problem of unsupervised domain adaptation, in the context of visual recognition. The proposed method – SALT – poses alignment as an auxiliary task to the primary task of maximizing performance on both source and target datasets. SALT proposes to solve domain alignment by utilizing gradients from the primary task. It utilizes an alternating optimization strategy, without refining the feature extractor, thus providing a venue for systematic control of domain alignment under the objective of generalizing to the target set. Through an extensive quantitative and qualitative evaluation, it is shown that SALT achieves comparable or sometimes higher performance than the state-of-the-art on

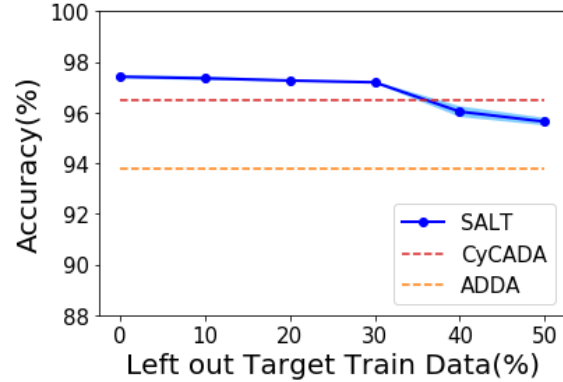


Figure 5: Performance on the target test-set with varying sizes of target training data on the USPS to MNIST adaptation task. The baseline results with ADDA and CyCADA were obtained using the entire target training data.

multiple benchmarks. Future work includes extending the SALT methodology to newer tasks such as semantic segmentation, open-set classification [39], and image-to-image translation.

References

- [1] Shai Ben-David, John Blitzer, Koby Crammer, Alex Kulesza, Fernando Pereira, and Jennifer Wortman Vaughan. A theory of learning from different domains. *Mach. Learn.*, 79(1-2):151–175, May 2010. 2
- [2] Bharath Bhushan Damodaran, Benjamin Kellenberger, Rémi Flamary, Devis Tuia, and Nicolas Courty. Deepjdot: Deep joint distribution optimal transport for unsupervised domain adaptation. In *Proceedings of the European Conference on Computer Vision (ECCV)*, pages 447–463, 2018. 7

- [3] Konstantinos Bousmalis, Nathan Silberman, David Dohan, Dumitru Erhan, and Dilip Krishnan. Unsupervised pixel-level domain adaptation with generative adversarial networks. In *Proceedings of the IEEE conference on computer vision and pattern recognition*, pages 3722–3731, 2017. 1
- [4] Nicolas Courty, Rémi Flamary, Devis Tuia, and Alain Rakotomamonjy. Optimal transport for domain adaptation. *IEEE Transactions on Pattern Analysis and Machine Intelligence*, 39:1853–1865, 2017. 4
- [5] Basura Fernando, Amaury Habrard, Marc Sebban, and Tinne Tuytelaars. Unsupervised visual domain adaptation using subspace alignment. In *IEEE International Conference on Computer Vision, ICCV 2013, Sydney, Australia, December 1-8, 2013* [5], pages 2960–2967. 1, 2, 3, 4, 9
- [6] Basura Fernando, Amaury Habrard, Marc Sebban, and Tinne Tuytelaars. Subspace alignment for domain adaptation. *CoRR*, abs/1409.5241, 2014. 2
- [7] Chelsea Finn, Pieter Abbeel, and Sergey Levine. Model-agnostic meta-learning for fast adaptation of deep networks. In *Proceedings of the 34th International Conference on Machine Learning-Volume 70*, pages 1126–1135. JMLR. org, 2017. 2
- [8] Geoffrey French, Michal Mackiewicz, and Mark H. Fisher. Self-ensembling for visual domain adaptation. In *The 6th International Conference on Learning Representations (ICLR)*, 2018. 3
- [9] Yaroslav Ganin and Victor Lempitsky. Unsupervised domain adaptation by backpropagation. *arXiv preprint arXiv:1409.7495*, 2014. 1
- [10] Yaroslav Ganin, Evgeniya Ustinova, Hana Ajakan, Pascal Germain, Hugo Larochelle, François Laviolette, Mario Marchand, and Victor Lempitsky. Domain-adversarial training of neural networks. *The Journal of Machine Learning Research*, 17(1):2096–2030, 2016. 1, 2, 5, 6, 7
- [11] Boqing Gong, Yuan Shi, Fei Sha, and Kristen Grauman. Geodesic flow kernel for unsupervised domain adaptation. *2012 IEEE Conference on Computer Vision and Pattern Recognition*, pages 2066–2073, 2012. 1, 2
- [12] Ian Goodfellow, Jean Pouget-Abadie, Mehdi Mirza, Bing Xu, David Warde-Farley, Sherjil Ozair, Aaron Courville, and Yoshua Bengio. Generative adversarial nets. pages 2672–2680, 2014. 2
- [13] Raghuraman Gopalan, Ruonan Li, and Rama Chellappa. Domain adaptation for object recognition: An unsupervised approach. *2011 International Conference on Computer Vision*, pages 999–1006, 2011. 2
- [14] Kaiming He, Xiangyu Zhang, Shaoqing Ren, and Jian Sun. Deep residual learning for image recognition. pages 770–778, 2016. 3, 5, 7
- [15] Judy Hoffman, Erik Rodner, Jeff Donahue, Kate Saenko, and Trevor Darrell. Efficient learning of domain-invariant image representations. In *1st International Conference on Learning Representations, ICLR 2013, Scottsdale, Arizona, USA, May 2-4, 2013, Conference Track Proceedings*, 2013. 1
- [16] Judy Hoffman, Eric Tzeng, Taesung Park, Jun-Yan Zhu, Phillip Isola, Kate Saenko, Alexei A. Efros, and Trevor Darrell. Cycada: Cycle-consistent adversarial domain adaptation. In *Proceedings of the 35th International Conference on Machine Learning, ICML 2018, Stockholm, Sweden, July 10-15, 2018* [16], pages 1994–2003. 1, 2, 7, 9
- [17] Jonathan J. Hull. A database for handwritten text recognition research. *IEEE Transactions on pattern analysis and machine intelligence*, 16(5):550–554, 1994. 7
- [18] Phillip Isola, Jun-Yan Zhu, Tinghui Zhou, and Alexei A Efros. Image-to-image translation with conditional adversarial networks. pages 1125–1134, 2017. 2
- [19] Max Jaderberg, Volodymyr Mnih, Wojciech Marian Czarnecki, Tom Schaul, Joel Z. Leibo, David Silver, and Koray Kavukcuoglu. Reinforcement learning with unsupervised auxiliary tasks. In *5th International Conference on Learning Representations, ICLR 2017, Toulon, France, April 24-26, 2017, Conference Track Proceedings*, 2017. 2
- [20] Diederik P Kingma and Jimmy Ba. Adam: A method for stochastic optimization. *arXiv preprint arXiv:1412.6980*, 2014. 6
- [21] Gregory Koch, Richard Zemel, and Ruslan Salakhutdinov. Siamese neural networks for one-shot image recognition. In *ICML deep learning workshop*, volume 2, 2015. 2
- [22] Yann LeCun, Corinna Cortes, and CJ Burges. Mnist handwritten digit database. *AT&T Labs [Online]*. Available: <http://yann.lecun.com/exdb/mnist>, 2:18, 2010. 7
- [23] Lukas Liebel and Marco Körner. Auxiliary tasks in multi-task learning. *CoRR*, abs/1805.06334, 2018. 2
- [24] Ming-Yu Liu, Thomas Breuel, and Jan Kautz. Unsupervised image-to-image translation networks. In I. Guyon, U. V. Luxburg, S. Bengio, H. Wallach, R. Fergus, S. Vishwanathan, and R. Garnett, editors, *Advances in Neural Information Processing Systems*, pages 700–708. Curran Associates, Inc., 2017. 2, 7
- [25] Ming-Yu Liu and Oncl Tuzel. Coupled generative adversarial networks. In *Advances in neural information processing systems*, pages 469–477, 2016. 1
- [26] Shikun Liu, Andrew J Davison, and Edward Johns. Self-supervised generalisation with meta auxiliary learning. *arXiv preprint arXiv:1901.08933*, 2019. 2
- [27] Mingsheng Long, Yue Cao, Jianmin Wang, and Michael I Jordan. Learning transferable features with deep adaptation networks. *arXiv preprint arXiv:1502.02791*, 2015. 4, 5, 6, 7
- [28] Mingsheng Long, Yue Cao, Jianmin Wang, and Michael I. Jordan. Learning transferable features with deep adaptation networks. In *Proceedings of the 32nd International Conference on International Conference on Machine Learning - Volume 37*, ICML’15, pages 97–105. JMLR.org, 2015. 7
- [29] Mingsheng Long, Zhangjie Cao, Jianmin Wang, and Michael I. Jordan. Conditional adversarial domain adaptation. In *Advances in Neural Information Processing Systems (NeurIPS)*, pages 1647–1657, 2018. 1, 2, 5, 6, 7
- [30] Mingsheng Long, Han Zhu, Jianmin Wang, and Michael I Jordan. Deep transfer learning with joint adaptation networks. In *Proceedings of the 34th International Conference on Machine Learning-Volume 70*, pages 2208–2217. JMLR. org, 2017. 5, 6, 7
- [31] Laurens van der Maaten and Geoffrey Hinton. Visualizing data using t-sne. *Journal of machine learning research*, 9(Nov):2579–2605, 2008. 8

- [32] Tsendsuren Munkhdalai and Hong Yu. Meta networks. In *Proceedings of the 34th International Conference on Machine Learning, ICML 2017, Sydney, NSW, Australia, 6-11 August 2017*, pages 2554–2563, 2017. 2
- [33] Yuval Netzer, Tao Wang, Adam Coates, Alessandro Bissacco, Bo Wu, and Andrew Y Ng. Reading digits in natural images with unsupervised feature learning. 2011. 7
- [34] Sinno Jialin Pan, Ivor W Tsang, James T Kwok, and Qiang Yang. Domain adaptation via transfer component analysis. *IEEE Transactions on Neural Networks*, 22(2):199–210, 2010. 2
- [35] Adam Paszke, Sam Gross, Soumith Chintala, Gregory Chanan, Edward Yang, Zachary DeVito, Zeming Lin, Alban Desmaison, Luca Antiga, and Adam Lerer. Automatic differentiation in pytorch. In *NIPS-W*, 2017. 5
- [36] Sachin Ravi and Hugo Larochelle. Optimization as a model for few-shot learning. In *5th International Conference on Learning Representations, ICLR 2017, Toulon, France, April 24-26, 2017, Conference Track Proceedings*, 2017. 2
- [37] Olga Russakovsky, Jia Deng, Hao Su, Jonathan Krause, Sanjeev Satheesh, Sean Ma, Zhiheng Huang, Andrej Karpathy, Aditya Khosla, Michael Bernstein, et al. Imagenet large scale visual recognition challenge. *International journal of computer vision*, 115(3):211–252, 2015. 5
- [38] Kate Saenko, Brian Kulis, Mario Fritz, and Trevor Darrell. Adapting visual category models to new domains. In *ECCV*, 2010. 2
- [39] Kuniaki Saito, Shohei Yamamoto, Yoshitaka Ushiku, and Tatsuya Harada. Open set domain adaptation by backpropagation. In *The European Conference on Computer Vision (ECCV)*, September 2018. 8
- [40] Swami Sankaranarayanan, Yogesh Balaji, Carlos D Castillo, and Rama Chellappa. Generate to adapt: Aligning domains using generative adversarial networks. In *Proceedings of the IEEE Conference on Computer Vision and Pattern Recognition*, pages 8503–8512, 2018. 7
- [41] Adam Santoro, Sergey Bartunov, Matthew Botvinick, Daan Wierstra, and Timothy Lillicrap. Meta-learning with memory-augmented neural networks. In *Proceedings of the 33rd International Conference on International Conference on Machine Learning - Volume 48, ICML’16*, pages 1842–1850. JMLR.org, 2016. 2
- [42] Ashish Shrivastava, Sumit Shekhar, and Vishal M Patel. Unsupervised domain adaptation using parallel transport on grassmann manifold. In *Applications of Computer Vision (WACV), 2014 IEEE Winter Conference on*, pages 277–284. IEEE, 2014. 1
- [43] Rui Shu, Hung Bui, Hirokazu Narui, and Stefano Ermon. A DIRT-t approach to unsupervised domain adaptation. In *International Conference on Learning Representations*, 2018. 1, 2, 3
- [44] Baochen Sun, Jiashi Feng, and Kate Saenko. Correlation alignment for unsupervised domain adaptation. In *Domain Adaptation in Computer Vision Applications*, pages 153–171. Springer, 2017. 2
- [45] Baochen Sun and Kate Saenko. Subspace distribution alignment for unsupervised domain adaptation. In *BMVC*, pages 24–1, 2015. 2
- [46] Baochen Sun and Kate Saenko. Deep coral: Correlation alignment for deep domain adaptation. In *European Conference on Computer Vision*, pages 443–450. Springer, 2016. 7
- [47] Kowshik Thopalli, Rushil Anirudh, Jayaraman J Thiagarajan, and Pavan Turaga. Multiple subspace alignment improves domain adaptation. In *ICASSP 2019-2019 IEEE International Conference on Acoustics, Speech and Signal Processing (ICASSP)*, pages 3552–3556. IEEE, 2019. 1
- [48] Shubham Toshniwal, Hao Tang, Liang Lu, and Karen Livescu. Multitask learning with low-level auxiliary tasks for encoder-decoder based speech recognition. In *Interspeech 2017, 18th Annual Conference of the International Speech Communication Association, Stockholm, Sweden, August 20-24, 2017*, pages 3532–3536, 2017. 2
- [49] Eric Tzeng, Judy Hoffman, Kate Saenko, and Trevor Darrell. Adversarial discriminative domain adaptation. In *Computer Vision and Pattern Recognition (CVPR)*, volume 1, page 4, 2017. 1, 7
- [50] Hemanth Venkateswara, Jose Eusebio, Shayok Chakraborty, and Sethuraman Panchanathan. Deep hashing network for unsupervised domain adaptation. pages 5018–5027, 2017. 7
- [51] Oriol Vinyals, Charles Blundell, Timothy Lillicrap, Daan Wierstra, et al. Matching networks for one shot learning. In *Advances in neural information processing systems*, pages 3630–3638, 2016. 2